# A2B: Neural Rendering of Ambisonic Recordings to Binaural

Israel D. Gebru, Todd Keebler, Jake Sandakly, Steven Krenn, Dejan Marković,
Julia Buffalini, Samuel Hassel, and Alexander Richard
*Codec Avatars Lab - Meta Reality Labs Research*, Pittsburgh PA, USA

***Abstract*—This paper introduces a novel neural network model for rendering binaural audio directly from ambisonic recordings. We optimized the model end-to-end to learn a direct mapping between ambisonic and binaural signals. Our approach eliminates traditional processing steps that were required to mitigate artifacts due to spherical harmonic order truncation and spatial aliasing, as well as other complex filtering needed to compensate for near-field sound sources. To showcase the advantage of neural network-based rendering over traditional signal processing approaches, we introduce a new dataset that includes challenging near-field sound sources, including speech and background noises. We demonstrate that our model can produce binaural audio results that closely match the fidelity of ground truth binaural recordings. Our comprehensive validation shows that the proposed method outperforms existing methods on several error metrics as well as in subjective evaluations. Model code, demos and datasets are available on our project webpage.**

***Index Terms*—ambisonics, spatial audio, binaural audio, neural rendering, spherical harmonics**

## I. Introduction

Spatial audio aims to provide listeners with appropriate spatial cues, delivering a convincing, engaging, and immersive audio experience. Rendering binaural signals from ambisonic recordings is one of the most accessible techniques to reproduce spatial audio. It is widely used in immersive multimedia applications [1], [2]. In virtual reality (VR), for example, this technique creates interactive audio experiences that complement visual elements; enhancing users' sense of immersion. The entertainment industry also employs this approach in music, film, and gaming to reproduce realistic sound scenes with depth and directionality cues.

Over the years, researchers have proposed numerous techniques for rendering binaural audio from ambisonic recordings [3]. Most of these methods, whether for headphones or loudspeaker setups, involve processing audio signals in the spherical harmonics domain and using head-related transfer functions (HRTFs). However, these rendering techniques often face constraints due to inherent limitations in both spherical harmonics and HRTFs.

Spherical harmonics processing, also known as ambisonic encoding and decoding, offers a mathematically powerful and convenient way to represent sound fields [4], [5]. However, sound fields described in spherical harmonics have a restricted spatial order due to hardware constraints or the need for efficient higher-order acoustic simulations. This restriction causes spatial aliasing within the spherical harmonics domain. Moreover, binaural rendering requires combining the sound field with an inherently high spatial order HRTF. This disparity leads to HRTF truncation, resulting in audible distortions in the binaural signal—such as coloration, poor localization, and low loudness stability [6], [7]. Additionally, ambisonic encoding and decoding assume virtual sources and loudspeakers radiate plane waves from the far field [8]. However, a notable limitation exists for binaural rendering of near sources: errors arise due to incorrect accounting for scattering. Near-field sources, defined as within 0.5–1.0m (or "within arm's reach"), have complex wave-front curvatures and frequency-dependent, highly non-linear distance-energy relationships.

Several techniques have been proposed to reduce spatial aliasing effects and distortions from HRTF order reduction [9], [10]. These aim to reduce the HRTFs' effective spatial order, resulting in less information lost during the truncation. For example, by aligning onsets [11] or disregarding HRTF phase above a given cutoff frequency, assuming it is perceptually irrelevant [10]. To address limitations for near-field rendering, solutions like near-field compensation filters [8] and additional plane-wave expansion [12] have been suggested. However, these approaches often rely on potentially inaccurate physical or psychoacoustic models and can be computationally demanding.

Recent neural network-based binaural rendering techniques show promise in overcoming conventional methods' limitations. These approaches can render binaural audio from various sources, including mono [13]–[16], first-order ambisonic signals [17], [18], and irregular arrays [19], [20]. Unlike traditional techniques, neural network models can learn complex non-linear functions and are not constrained by linear filters like HRTFs or linear processing using spherical harmonics transforms. Moreover, while traditional techniques often prioritize retaining perceptually important information; end-to-end models are optimized directly based on rendering results, potentially preserving more nuanced information.

Inspired by recent progress in neural network-based binaural audio rendering research, we propose a novel waveform-domain neural network model for rendering binaural audio from raw ambisonic recordings. Our model extracts sound-field information from individual channels of the raw ambisonic recordings, enabling accurate reproduction regardless of sound source type, direction, or position. By optimizing the model end-to-end, we learn a direct mapping between ambisonic and binaural signals. This approach effectively handles near-field

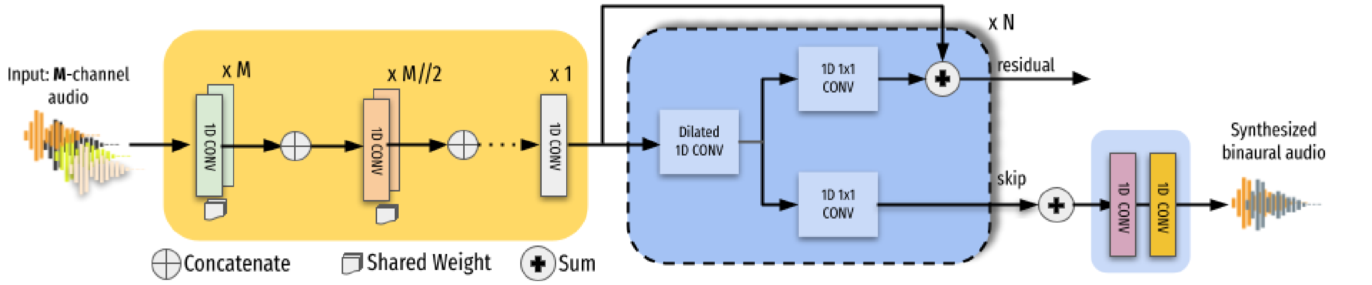


**Fig. 1:** Our proposed model architecture. Given M-channel ambisonic audio, each channel is passed through a shared 1D conv network and then concatenated. We progressively scale-down the feature dimensions using shared 1D conv networks until the desired feature dimension is achieved. These features pass through N residual blocks. The averaged skip outputs are processed by a small 1D conv network to produce the binaural waveform. Nonlinear activation/dropout layers are omitted for simplicity.

rendering without cumbersome compensation heuristics and generates background/diffuse noise sounds that closely match ground truth binaural recordings. Our modeling technique avoids frequency domain representation, instead modeling phase information directly in the waveform domain. This allows for accurate interaural time difference (ITD) prediction and offers the flexibility to use head-tracking to rotate the scene before binaural rendering. In contrast to [17], [18], we have a fully real-time approach using convolutional neural networks.

We benchmarked our model on two public available datasets [17], [21]. To address near-field rendering challenges, we collected more than 20 hours of data simultaneously with binaural microphone and higher-order ambisonic microphones ($10^{\text{th}}$-, $4^{\text{th}}$- and $2^{\text{nd}}$-order). Using this data, we conducted a systematic study to highlight the benefits of end-to-end optimization over conventional methods, particularly in rendering near-field sources and reproducing background sounds. The proposed model code, dataset, and results are publicly available on our project webpage.[1]

The remainder of this paper is organized as follows: Section II presents the proposed model and network architecture. Section III reviews existing datasets and introduces our new dataset for data-driven ambisonics-to-binaural rendering. Section IV details the experimental setup. Section V presents the quantitative and qualitative performance of our method compared to existing approaches. Finally, Section VI concludes the paper.

## II. Proposed Model

We propose an end-to-end model that takes raw ambisonic recordings and outputs the corresponding binaural signals. Given ambisonic recordings $\boldsymbol{x}_a \in \mathbb{R}^{\mathrm{M}\times\mathrm{T}}$ of length T and M number of channels, our goal is to generate the corresponding binaural audio $\boldsymbol{y} \in \mathbb{R}^{2\times\mathrm{T}}$ as: $\mathcal{F}(\boldsymbol{x}_a;\boldsymbol{\theta}) \mapsto \boldsymbol{y}$, where $\mathcal{F}$ denotes the ambisonic to binaural transformation function parameterized by the weights $\boldsymbol{\theta}$ of our neural network.

We assume that $\mathcal{F}$ models the overall rendering from multi-channel audio recording to binaural. In the convectional approach $\mathcal{F}$ could represent the signal processing pipeline which include spherical harmonics encoding and decoding, HRTF filtering and other handcrafted and manually tuned parameters like diffuse field equalization [22], [23] and near-field compensation filters [8], [12], [24].

The model architecture is show in Figure 1 and described as follows. We build the network based on a bidirectional dilated convolution architecture that is different from WaveNet [25] because there is no auto-regressive constraints. The network composed of a three main sub-modules. The first sub-module is the waveform encoder, which processes the raw waveform and produces C channels of intermediate features. These features maintain the same temporal resolution as the input signal. Given that the input consists of multichannel audio, we treat each channel as a distinct image of the sound scene. Instead of using a multichannel convolution layer, we employ shared 1D convolution layers and concatenate the output from multiple channels in the channel dimension. This helps to find the inter-channel relationship between signals recorded by different microphones.

The second sub-module consists of a stack of $N$ Residual layers with $C$ residual channels. These layers are grouped into $b$ blocks, each containing $n = N/b$ layers. We employ a bi-directional dilated convolution with a kernel size of 3 in each layer. The dilation doubles with each layer within a block, i.e. $[1, 2, 4, \cdots, 2^{n-1}]$. We then average all skip outputs from the residual blocks. The third sub-module, a compact two-layer 1D convolution network, processes the mean of these skip-connection features and outputs a two-channel waveform.

## III. Paired Ambisonic-Binaural Datasets

Our data-driven approach required paired ambisonic and binaural audio recordings. This section briefly outlines existing ambisonic-binaural audio datasets and introduces our novel dataset, namely the **A2B** (**A**mbisonic to **B**inaural) dataset.

### A. Public Datasets

To the best of our knowledge, only two publicly available datasets exist: the ByteDance Paired Ambisonic and Binaural (BTPAB) dataset [17] and the Urban Soundscape dataset [21]. BTPAB contains 49 minutes of a music band recorded in anechoic chamber using a first-order ambisonics microphone and a Neumann KU100 binaural head. The Urban Soundscape, originally collected for urban sounds classification, offers

[1] https://github.com/facebookresearch/A2B

| Dataset Name | Seq. Name | Environment | Content | Amb. Order(#Mic) | Length(hr) | Offset(meters) | NF | FF |
|---|---|---|---|---|---|---|---|---|
| UrbanSounds [21] | - | Outdoor/multiple cities | Outdoor noises | 1(4) | 2.21 | 0.4 | ✗ | ✓ |
| BTPAB [17] | - | Anechoic | Music | 1(4) | 0.49 | 0.01 | ✗ | ✓ |
| A2B (Ours) | 10-A2B-R1 | Semi-Anechoic | Speech | 10(128) | 10.11 | 0.04 | ✗ | ✓ |
| | 10-A2B-R2 | Standard Room | Speech | 10(128) | 10.32 | 0.01 | ✓ | ✓ |
| | 4-A2B-MP | Semi-Anechoic | Music and Speech | 4(32) | 6.53 | 0.0 | ✓ | ✓ |
| | 2-A2B-MP | Semi-Anechoic | Music and Speech | 2(8) | 6.53 | 0.0 | ✓ | ✓ |

**TABLE I:** Summary of Paired Ambisonic-Binaural Datasets. Offset is the closest distance between the binaural head and the ambisonic microphone. NF and FF columns show if the dataset contains near- and far-field sounds sources, respectively.

diverse sounds from cities around the world. It is recorded using first-order ambisonics microphone and HEAD acoustics binaural head, positioned 40cm apart vertically. This height difference complicates ambisonic to binaural mapping problem due to significant signal variations. Table I provides additional details on these datasets.

### *B. Proposed **A2B** Dataset*

To address the lack of datasets for training and testing neural rendering performance on near-field sounds and higher-order ambisonics, we created a new dataset using higher-order ambisonics microphones and binaural mannequins (HATS and KEMAR). We named this dataset **A2B** (**A**mbisonic to **B**inaural). The dataset covers various acoustic environments, including near-field scenarios and varying numbers of sound sources, encompassing speech and background noises recorded simultaneously with a binaural microphone paired with a higher-order ambisonic microphone. We used $10^{\text{th}}$-, $4^{\text{th}}$- and $2^{\text{nd}}$-order ambisonic microphones.

We collected the **A2B** dataset in two different acoustic settings. The first was in a semi-anechoic chamber with both sensors positioned in the middle and a group of people speaking within a $1.0m$ radius. The second was a noisy room with significant background noise from multiple AC vents, home appliances and a nearby busy street. In all recordings, we positioned the ambisonic microphone atop of HATS mannequin, leaving about 1cm of space between the top of the head and the lowest point of the ambisonic microphone. Our dataset features 2 to 5 people in group conversations. We recorded a total of 16 different individuals. More details about the dataset capture setup is shown in Figure 2.

All datasets mentioned have positional offsets between ambisonic and binaural microphone, which causes sound field mismatches. While end-to-end approaches can adapt to these mismatches, they disadvantage conventional rendering techniques when comparing synthesized outputs to ground-truth binaural signals. To create perfectly matched recordings, we generated reproducible sound scenes using an ambisonic loudspeaker array. We used speech from the VCTK dataset [26] and in-house music data, and created spatialized audio scenes with random walk patterns via the Spat5 library [27]. We recorded these scenes three times: with a binaural head, then second-order and fourth-order ambisonic microphones at the center. We used laser guides to ensure precise positioning.

Our dataset comprises four parts: “10-A2B-R1” and “10-A2B-R2” (10th-order recordings in semi-anechoic and noisy environments), and “4-A2B-MP” and “2-A2B-MP” (4th and 2nd-order recordings in semi-anechoic room with matching sensor positions). We believe the **A2B** dataset could serve as a valuable resource for training and benchmarking data-driven ambisonic-to-binaural mapping techniques. The dataset will be publicly available.

## IV. Experiments

### *A. Implementation Details*

**Loss Functions**: We train the proposed model by minimizing point-wise L2 loss on the raw waveform $\mathcal{L}_2$ and different STFT based losses in time-frequency domain $H = |\text{STFT(y)}|$, including spectral converges loss $\mathcal{L}_{\text{sc}}$ and magnitude difference loss $\mathcal{L}_{\text{mag}}$:

$$\begin{aligned}\mathcal{L}_{\text{total}} &= \lambda_{\text{l2}}\ \mathcal{L}_2 + \lambda_{\text{sc}}\ \mathcal{L}_{\text{sc}} + \lambda_{\text{mag}}\ \mathcal{L}_{\text{mag}} \\ &= \lambda_{\text{l2}}\ \|\hat{y} - y\|_2 + \lambda_{\text{sc}} \frac{\|\hat{H} - H\|_2}{\|H\|_2} + \lambda_{\text{mag}} \|\hat{H} - H\|_1.\end{aligned}$$

We used multi-resolution STFT [28], which involves computing an STFT loss at multiple time-frequency scales. In all experiments, we set FFT size as $\{128, 512, 1024, 2048\}$, window length as $\{80, 240, 600, 1200\}$, and hop length as $\{16, 50, 120, 240\}$. We set $\lambda_{\text{l2}} = 20.0$, $\lambda_{\text{sc}} = 1.0$ and $\lambda_{\text{mag}} = 10.0$.

**Model Training**: We trained and tested our model on A2B, BTPAB [17] and UrbanSounds [21] datasets. For A2B dataset and UrbanSounds, we use 80% of the data for training and hold out 5% and 15% for validation and testing, respectively. For BTPAB dataset we followed the train/test spit as used in [17]. We used AdamW optimizer (learning rate $10^{-4}$) and batch size 32. Models were trained on two NVIDIA H100 GPUs for 400k steps and evaluated on the last epoch.

### *B. Baselines*

We compare our model with the neural network model proposed for the BTPAB dataset [17]. This is the only directly comparable pre-existing baseline. We used the highest-performing model, **SCGAD**, as reported in [17] as our baseline. To compare with traditional approach, we adopted the rendering pipeline **MagLS** proposed in [29] and used their open-source reference implementation.

### *C. Model Evaluation Metrics*

Following [17], we used several metrics to asses the quality of the predicted binaural audio. We measure performance from two aspects: (1) closeness to the ground truth as measured by the SDR (Signal-to-Distortion ratio). (2) correctness of the spatial sound as measured by DILD (Difference in

(a) (b) (c) (d)

**Fig. 2:** Dataset collection setup for **A2B** dataset. (a) recording setup with a $10^{\text{th}}$ order ambisonic microphone and binaural mannequin (B+K HATS), (b) participants during recording in the semi-anechoic room, (c) participants during recording in the "normal" room, (d) loudspeaker array recording setup for matching position (*-MP) portions of our dataset.

| Model | SDR (dB) ↑ | DILD (dB) ↓ | DITD (ms) ↓ | # Params ($10^6$) |
|---|---|---|---|---|
| SCGAD [17] | 8.300 | 9.650 | 0.520 | 593 |
| MagLS [29] | -1.490 | 15.65 | 1.180 | - |
| Ours | **11.022** | **1.483** | **0.042** | 0.700 |

**TABLE II:** Performance comparison of our proposed model with existing methods on the BTPAB dataset [17]. The results are averaged across all test recordings. The best results are in **bold**.

| Dataset | Model | SDR (dB) ↑ | DILD (dB) ↓ | DITD (ms) ↓ | LRE ↓ |
|---|---|---|---|---|---|
| UrbanSounds | Ours | 10.807 | 2.1974 | 3.875 | 0.408 |
| 10-A2B-R1 | Ours | 5.805 | 1.166 | 0.102 | 0.214 |
| 10-A2B-R2 | Ours | 9.867 | 1.486 | 0.064 | 0.330 |
| 4-A2B-MP | MagLS [29] | -1.756 | 3.956 | 0.204 | 1.267 |
| | Ours | **7.270** | **1.571** | **0.071** | **0.180** |
| 2-A2B-MP | MagLS [29] | -3.667 | 2.617 | 2.469 | 2.016 |
| | Ours | **2.943** | **1.907** | **0.097** | **0.220** |

**TABLE III:** The performance of our proposed model on Urbansound and A2B datasets. We omitted MagLS [29] results on Urbansound, 10-A2B-R1 and 10-A2B-R2, as it would not be a fair comparison.

Interaural Level Difference), DILD (Difference in Interaural Time Difference) and by LRE (left-right energy ratio error) as defined in [30]. Higher SDR and lower DILD and LRE values indicate a good match in energy compared to the ground truth, while higher DITD implies incorrect time delays in the binaural signal, hence wrong spatialzations.

### D. Subjective Evaluation

We conducted a subjective evaluation based on MUSHRA (Multiple Stimuli with Hidden Reference and Anchor) [31] to assess our model's perceptual quality versus ground-truth recordings. We followed a similar protocol and rating as used it [32]. We asked 11 people to rate the audio similarity and spatialization quality by comparing audio examples from our model against a traditional magLS [29] approach. They were asked to rate on a scale ranging from 0 (unrecognizable) to 100 (perfect). To ensure a fair comparison with the traditional method, we limited listening tests to results on "4-A2B-MP" and "2-A2B-MP" of the A2B datasets. For all others, we reported quantitative results.

## V. Results and Discussions

**Quantitative Results**: Table II summerize the result of our proposed model compared to the baseline SCGAD model proposed in [17]. Our model outperform SCGAD in all metrics while being $900\times$ smaller in model parameters.

We compare our proposed model with the traditional ambisonic rendering technique MagLS [29] on a portion of the A2B dataset that contains matched sound scenes. The results, as presented in Table III, demonstrate that our proposed model consistently outperforms MagLS across all metrics. Interestingly, our proposed model and MagLS exhibited improved performance as the order of ambisonics increased from 2 to 4. This trend aligns with expectations, as higher-order ambisonics provide a more detailed spatial representation of the sound field, ultimately leading to improved binaural rendering quality.

| Dataset | Model | Audio Similarity ↑ | Spatialization Quality ↑ |
|---|---|---|---|
| 4-A2B-MP | MagLS [29] | $29.35 \pm 18.43$ | $34.76 \pm 18.89$ |
| | Ours | $69.1 \pm 17.61$ | $79.06 \pm 13.02$ |
| | Rec | $82.13 \pm 12.96$ | $87.73 \pm 11.11$ |
| 2-A2B-MP | MagLS [29] | $17.02 \pm 13.98$ | $24.76 \pm 17.97$ |
| | Ours | $79.57 \pm 15.12$ | $85.39 \pm 12.91$ |
| | Rec | $85.74 \pm 11.60$ | $90.28 \pm 9.837$ |

**TABLE IV:** Subjective evaluations of our model compared to conventional MagLS [29] approach. "Rec" indicates that the actual recordings were used as one of the hidden test signals.

**Subjective Results**: The results from the listening evaluation are shown in Table IV. For both audio similarity and spatialization scores, listeners gave higher ratings to the ground-truth recordings. This was expected since we duplicated the actual recording as a hidden test signal. Our proposed model's results were rated statistically competitive with the ground-truth recordings but significantly higher compared to the results from the baseline traditional method MagLS. Listeners commented that they can easily discerned the difference between MagLS results and the reference signals.

## VI. Conclusion

In this paper, we have introduced a novel waveform model for rendering high-fidelity binaural audio directly from raw ambisonic recordings. Our approach employs end-to-end optimization techniques to learn a direct, efficient mapping between ambisonic and binaural signals. This eliminates the need for complex heuristics typically required in traditional rendering methods, streamlining the process and potentially enhancing accuracy. Our experiments demonstrate consistent, accurate results across various sound scenes, including challenging near-field sources. This data-driven method could adapt to different microphone array configurations beyond ambisonics, such as smart glasses, multi-microphone smartphones, or custom arrays where binaural microphones or heads cannot be accommodated during testing.

## REFERENCES


[1] F. Zotter and M. Frank, *Ambisonics: A practical 3D audio theory for recording, studio production, sound reinforcement, and virtual reality*. Springer Nature, 2019.

[2] F. Olivieri, N. Peters, and D. Sen, "Scene-based audio and higher order ambisonics: A technology overview and application to next-generation audio, vr and 360 video," *EBU Tech*, 2019.

[3] B. Rafaely, V. Tourbabin, E. Habets, Z. Ben-Hur, H. Lee, H. Gamper, L. Arbel, L. Birnie, T. Abhayapala, and P. Samarasinghe, "Spatial audio signal processing for binaural reproduction of recorded acoustic scenes–review and challenges," *Acta Acustica*, vol. 6, p. 47, 2022.

[4] B. Rafaely, *Fundamentals of spherical array processing*. Springer, 2015, vol. 8.

[5] J. Ahrens, "Binaural audio rendering in the spherical harmonic domain: A summary of the mathematics and its pitfalls," *arXiv preprint arXiv:2202.04393*, 2022.

[6] A. Avni, J. Ahrens, M. Geier, S. Spors, H. Wierstorf, and B. Rafaely, "Spatial perception of sound fields recorded by spherical microphone arrays with varying spatial resolution," *The Journal of the Acoustical Society of America*, vol. 133, no. 5, pp. 2711–2721, 2013.

[7] Z. Ben-Hur, D. L. Alon, B. Rafaely, and R. Mehra, "Loudness stability of binaural sound with spherical harmonic representation of sparse head-related transfer functions," *EURASIP Journal on Audio, Speech, and Music Processing*, vol. 2019, pp. 1–14, 2019.

[8] J. Daniel, "Spatial sound encoding including near field effect: Introducing distance coding filters and a viable, new ambisonic format," in *Audio Engineering Society Conference: 23rd International Conference: Signal Processing in Audio Recording and Reproduction*. Audio Engineering Society, 2003.

[9] M. Zaunschirm, C. Schörkhuber, and R. Höldrich, "Binaural rendering of ambisonic signals by head-related impulse response time alignment and a diffuseness constraint," *The Journal of the Acoustical Society of America*, vol. 143, no. 6, pp. 3616–3627, 2018.

[10] C. Schörkhuber, M. Zaunschirm, and R. Höldrich, "Binaural rendering of ambisonic signals via magnitude least squares," in *Proceedings of the DAGA*, vol. 44, 2018, pp. 339–342.

[11] Z. Ben-Hur, D. L. Alon, R. Mehra, and B. Rafaely, "Binaural reproduction based on bilateral ambisonics and ear-aligned hrtfs," *IEEE/ACM Transactions on Audio, Speech, and Language Processing*, vol. 29, pp. 901–913, 2021.

[12] D. Menzies and M. Al-Akaidi, "Nearfield binaural synthesis and ambisonics," *The Journal of the Acoustical Society of America*, vol. 121, no. 3, pp. 1559–1563, 2007.

[13] A. Richard, D. Markovic, I. D. Gebru, S. Krenn, G. A. Butler, F. Torre, and Y. Sheikh, "Neural synthesis of binaural speech from mono audio," in *International Conference on Learning Representations*, 2021.

[14] I. D. Gebru, D. Marković, A. Richard, S. Krenn, G. A. Butler, F. De la Torre, and Y. Sheikh, "Implicit hrtf modeling using temporal convolutional networks," in *ICASSP 2021-2021 IEEE International Conference on Acoustics, Speech and Signal Processing (ICASSP)*. IEEE, 2021, pp. 3385–3389.

[15] Y. Leng, Z. Chen, J. Guo, H. Liu, J. Chen, X. Tan, D. Mandic, L. He, X. Li, T. Qin *et al.*, "Binauralgrad: A two-stage conditional diffusion probabilistic model for binaural audio synthesis," *Advances in Neural Information Processing Systems*, vol. 35, pp. 23 689–23 700, 2022.

[16] W. C. Huang, D. Markovic, A. Richard, I. D. Gebru, and A. Menon, "End-to-end binaural speech synthesis," *arXiv preprint arXiv:2207.03697*, 2022.

[17] Y. Zhu, Q. Kong, J. Shi, S. Liu, X. Ye, J.-C. Wang, H. Shan, and J. Zhang, "End-to-end paired ambisonic-binaural audio rendering," *IEEE/CAA Journal of Automatica Sinica*, vol. 11, no. 2, pp. 502–513, 2024.

[18] Y. Zhu, Q. Kong, J. Shi, S. Liu, X. Ye, J.-c. Wang, and J. Zhang, "Binaural rendering of ambisonic signals by neural networks," *arXiv preprint arXiv:2211.02301*, 2022.

[19] M. Heikkinen, A. Politis, and T. Virtanen, "Neural ambisonics encoding for compact irregular microphone arrays," in *ICASSP 2024-2024 IEEE International Conference on Acoustics, Speech and Signal Processing (ICASSP)*. IEEE, 2024, pp. 701–705.

[20] Y. Hsu, C. Ma, and M. R. Bai, "Model-matching principle applied to the design of an array-based all-neural binaural rendering system for audio telepresence," in *ICASSP 2023-2023 IEEE International Conference on Acoustics, Speech and Signal Processing (ICASSP)*. IEEE, 2023, pp. 1–5.

[21] K. Sun, B. De Coensel, K. Filipan, F. Aletta, T. Van Renterghem, T. De Pessemier, W. Joseph, and D. Botteldooren, "Classification of soundscapes of urban public open spaces," *Landscape and urban planning*, vol. 189, pp. 139–155, 2019.

[22] T. McKenzie, D. Murphy, and G. Kearney, "Directional bias equalization of first-order binaural ambisonic rendering," in *Audio Engineering Society Conference: 2018 AES International Conference on Audio for Virtual and Augmented Reality*. Audio Engineering Society, 2018.

[23] T. McKenzie, D. T. Murphy, and G. C. Kearney, "Diffuse-field equalisation of first-order ambisonics," in *Proc. 20th International Conference on Digital Audio Effects*, 2017.

[24] D. Romblom and B. Cook, "Near-field compensation for hrtf processing," in *Audio Engineering Society Convention 125*. Audio Engineering Society, 2008.

[25] A. v. d. Oord, S. Dieleman, H. Zen, K. Simonyan, O. Vinyals, A. Graves, N. Kalchbrenner, A. Senior, and K. Kavukcuoglu, "Wavenet: A generative model for raw audio," *arXiv preprint arXiv:1609.03499*, 2016.

[26] C. Veaux, J. Yamagishi, and S. King, "The voice bank corpus: Design, collection and data analysis of a large regional accent speech database," in *2013 international conference oriental COCOSDA held jointly with 2013 conference on Asian spoken language research and evaluation (O-COCOSDA/CASLRE)*. IEEE, 2013, pp. 1–4.

[27] T. Carpentier, "A new implementation of spat in max," in *15th Sound and Music Computing Conference (SMC2018)*, 2018, pp. 184–191.

[28] R. Yamamoto, E. Song, and J.-M. Kim, "Parallel wavegan: A fast waveform generation model based on generative adversarial networks with multi-resolution spectrogram," in *ICASSP 2020-2020 IEEE International Conference on Acoustics, Speech and Signal Processing (ICASSP)*. IEEE, 2020, pp. 6199–6203.

[29] T. Deppisch, H. Helmholz, and J. Ahrens, "End-to-end magnitude least squares binaural rendering of spherical microphone array signals," in *2021 Immersive and 3D Audio: from Architecture to Automotive (I3DA)*. IEEE, 2021, pp. 1–7.

[30] C. Chen, A. Richard, R. Shapovalov, V. K. Ithapu, N. Neverova, K. Grauman, and A. Vedaldi, "Novel-view acoustic synthesis," in *Proceedings of the IEEE/CVF Conference on Computer Vision and Pattern Recognition*, 2023, pp. 6409–6419.

[31] I. Recommendation *et al.*, "Method for the subjective assessment of intermediate quality level of coding systems," *ITU-R BS*, pp. 1534–1, 2003.

[32] H. Caracalla and A. Roebel, "Sound texture synthesis using ri spectrograms," in *ICASSP 2020-2020 IEEE International Conference on Acoustics, Speech and Signal Processing (ICASSP)*. IEEE, 2020, pp. 416–420.